JCEC
THE JOURNAL OF ENGINEERING AND EXACT SCIENCES

OPEN ACCESS

The Journal of Engineering and Exact Sciences – jCEC, Vol. 10 N. 04 (2024)
journal homepage: https://periodicos.ufv.br/jcec
eISSN: 2527-1075
ISSN: 2446-9416

Numerical modeling of RC column reinforced by new strategy using fiberglass tape and cloth

Article Info:
Article history: Received 2024-02-02 / Accepted 2024-05-13 / Available online 2024-05-13
doi: 10.18540/jcecvl10iss4pp18334

Aissa Boumedjane
ORCID: https://orcid.org/0009-0000-7026-8684
Laboratory of Research in Applied Hydraulics, LRHYA, Department of Civil Engineering, Faculty of Technology, University of Batna 2, Algeria,
LGC-ROI, Department of Civil Engineering Faculty of Technology University of Batna 2, Batna, Algeria
E-mail: a.boumedjane@univ-batna2.dz
Mohamed Saadi
ORCID: https://orcid.org/0000-0002-3495-5759
LGC-ROI, Department of Civil Engineering Faculty of Technology University of Batna 2, Batna, Algeria
E-mail: m.saadi@univ-batna2.dz
Djarir Yahiaoui
ORCID: https://orcid.org/0000-0003-4360-5600
LGC-ROI, Department of Civil Engineering Faculty of Technology University of Batna 2, Batna, Algeria
E-mail: d.yahiaoui@univ-batna2.dz
Noureddine Lahbari
ORCID: https://orcid.org/0000-0001-9468-0673
LGC-ROI, Department of Civil Engineering Faculty of Technology University of Batna 2, Batna, Algeria
E-mail: n.lahbari@univ-batna2.dz

Abstract
This paper presents the results of finite element analysis (FE) to study the axial compression behavior of reinforced concrete columns wrapped with tapes and fiberglass cloths according to different techniques using ABAQUS software. In the beginning, columns are modeled as 3D solid elements with a concrete damage plasticity model (CDPM), as the columns in this study are considered to be low compressive strength reinforced concrete and the rebar as 3D mesh elements. And once assembled, the specimen is wrapped with tape and cloth in the form of three-dimensional shell elements. Then, in order to analyze the behavior of the ultimate loads, the deformation of the confinement material, and the distribution of deformations in the concrete, the controlled displacement method used to apply the uniaxial compression loads to the specimen. Finally, a new mixed confinement model between partial confinement and complete has been proposed using a database of the results of a numerical simulation for confined concrete by fiberglass tapes and cloths. And it was found that the confinement strategy proposed in this study is very effective for the behavior of the reinforced concrete column, as the stress decreases significantly with the expansion and widening of the confinement stiffness of concrete in the plastic phase which improves the axial stress resistance.

Keywords: FRP, Column, Partially, Entirely, Confined concrete, Analysis, Confinement Fiberglass tape, Fiberglass cloth.

1. Introduction

Over the past decade, the escalating frequency and intensity of earthquakes have compelled engineers and researchers to embark on a comprehensive exploration of seismic structural behavior. This heightened focus has fueled investigations into various facets of earthquake engineering, encompassing:

- Delineating the differential effects of near-fault and far-fault earthquakes on structures and near-fault earthquakes that occur close to a ruptured fault line, also show distinct characteristics compared to distal-fault earthquakes that originate farther away. Which makes clarifying these differences extremely important for designing earthquake-resistant structures (Lemsara *et al*., 2023).

Unraveling the intricate interplay between soil-structure interaction (SSI) and structural behavior where refers to the dynamic interaction between a structure and the underlying soil. Comprehending and accounting for soil-structure interaction is essential for accurate structural analysis and design (Guettafi *et al*., 2022; Houda *et al*., 2018; Nesrine *et al*., 2021; Sekhri *et al*., 2020 and Souheyla & Djarir., 2022).

-Pioneering innovative techniques for structural strengthening and rehabilitation where engineers have devised various methodologies to enhance the seismic resilience of existing structures. They include retrofitting with bracing where bracing systems, comprising beams and struts are strategically employed to reinforce structural walls and frames (Abdelhamid *et al*., 2022, Saadi & Yahiaoui, 2022 and Yahiaoui *et al*., 2022) And using the concrete confinement by FRP composites composed of fiber-reinforced polymers, utilized to strengthen concrete columns and beams (Yahiaoui *et al*., 2023; and Yahiaoui *et al*., 2022).

Many factors can affect the results of reinforcement with FRPs materials and to investigate these factors Tan *et al*. (2013) conducted a research on concrete columns reinforced with fiber reinforced polymeric cloth under the influence of axial load and concluded that the number of cloth layers increases the bending capacity of the reinforced column, but the effect of the number of layers becomes negative when a limited number of layers is used due to the deterioration of the property of adhesion between them. While Hussain *et al*. (2016) investigated the behavior of circular and square columns confined by sprayed fiber reinforced polymer composites and concluded that the strength and ductility of confining materials increase more in circular columns and hence the square negatively affects the reinforcement, which made Tan *et al*. (2013) used in his study a column confinement model in which the rectangular shape closer to the circular shape, in order to give better confinement results. This and was mentioned by Benzaid *et al*. (2008) to improve containment efficiency and reduce the detrimental effect of the right angle on tensile failure such that these right angles must be bent. While Yang *et al*., 2020 and Zeng *et al*., 2018 used FRP strips in their reinforcement of columns and showed the effectiveness of this method of containment, and the effect of the distance between the strips and their thickness and width. It was also combined the partial confinement by FRP strips with the full confinement by FRP cloth according to the method Zeng *et al*. (2017), and there was a marked increase in the results of the study. While Guo *et al*. (2019) studied the methods of sticking the strips on the outer surface of the columns, such as there was a spiral and circular shape sticking. And it proved the difference in results and the extent of the effect of the wrap method on the effectiveness of reinforcement. And it was adopted Obaidat *et al*. (2020) a new method of reinforcement, by digging the grooves on the outer surface of the column to be reinforced, and they reached a relationship between the depth of the grooves, the distance between them and number folds.

From the above, one may wonder how to significantly increase the compressive capacity of confined concrete with the help of fiberglass cloth, in order to become the results of the latter close to reinforcement results at using a carbon fiber reinforced polymer. Although the strength of carbon fibers is not comparable to that of glass fibers, the load-deflection response of columns reinforced with glass fiber reinforced polymer can be improved through increasing the number of reinforcing layers, but this time, It was adopted this increase with a different technique to the traditional method so it was proposed strips of fiberglass cloth in the shape of a spiral was glued on the outer surface of the pole with the change parameter of number this constitutes a partial containment followed by

a full containment with the fiberglass cloth, also taking into account the criterion of the number of layers.

A numerical simulation with nonlinear analysis in ABAQUS was assigned for this study, and the behavior of a concrete column was analyzed by five distinct conditions for three different types of concrete with low compressive strengths of 5, 10, and 15 MPa.

2. Methodology

2.1 Design of test specimens

This study was conducted on three different types of concrete with low compressive strength 5, 10 and 15 MPa. The study specimens were considered as columns embedded and loaded at the other end of dimensions (200, 300 and 2000) mm, with longitudinal reinforcement bars 4 d 12 mm, and transverse D 6 mm in the form of stirrups with spacing between centers 100 mm for the plastic hinge region and 150 mm outside the plastic hinge region. All the geometric characteristics of the columns are shown in Figure 1. The slenderness effect of the column is not taken into account because it is a secondary effect in this geometry.

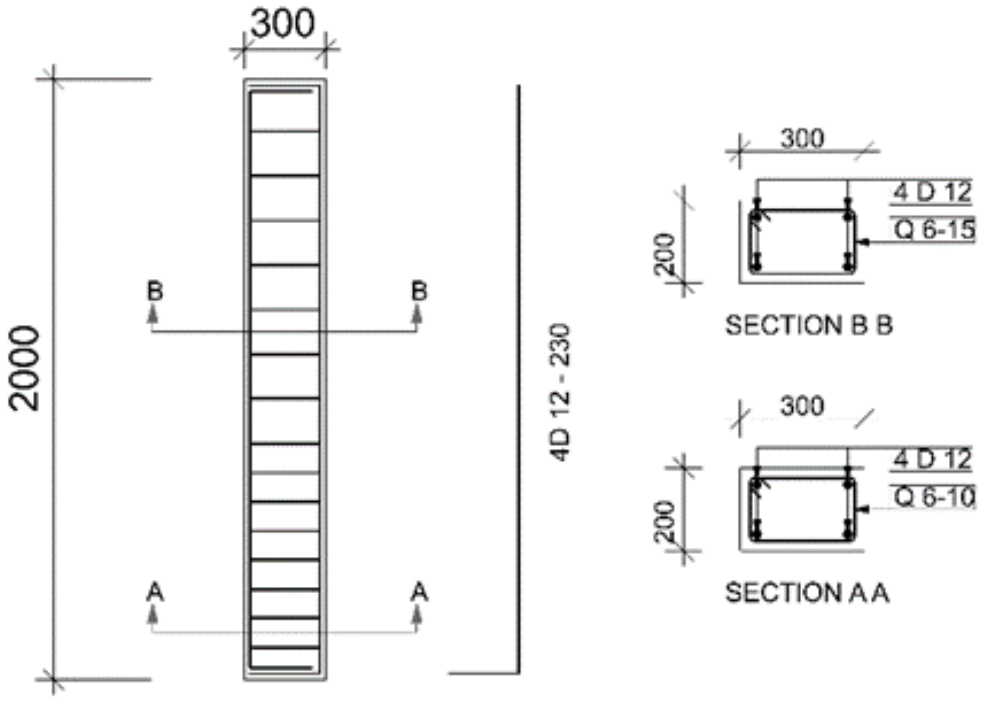

Figure 1 – The detail geometry of the specimen and a cross-sectional area.

The specimens were divided into 5 groups as shown in Table 1.

Table 1 – Variable types of specimens.

Specimen	Compressive strength / MPa	Axial displacement / mm	description
C1 C	5 10 15	50	Column 1 - Concrete Column
C2 RC	5 10 15	50	Column 2 - Reinforced concrete column
C3 RC-2S	5 10 15	50	Column 3 - Reinforced concrete column wrapped with two layers of fiberglass tape
C4 RC-2 S-2F	5 10 15	50	Column 4 - Reinforced concrete column wrapped with two layers of fiberglass tape and two layers of fiberglass cloth
C5 RC-2S-4F	5 10 15	50	Column 5 - Reinforced concrete column wrapped with two layers of fiberglass tape and four layers of fiberglass cloth

The confinement in this study ensured with two types, where the column of the third series (C3 RC-2S) reinforced by two layers of fiberglass tapes glued over the entire height of the outer facets of the column in spiral form as shown in Figure 2a, with a circular strapping at the start and terminus of tape to form hoops so as not to detach this latter at the beginning of the loading application. The columns of the fourth and fifth series (C4RC-2S-2F), (C5RC-2S-4F) successively, reinforced by two layers of fiberglass tape plus to two- or four-layers fiberglass cloth along the entire length of the column, as shown in Figures 2b and 2c. Installation details for the fiberglass tape and cloth are shown in Figure 2.

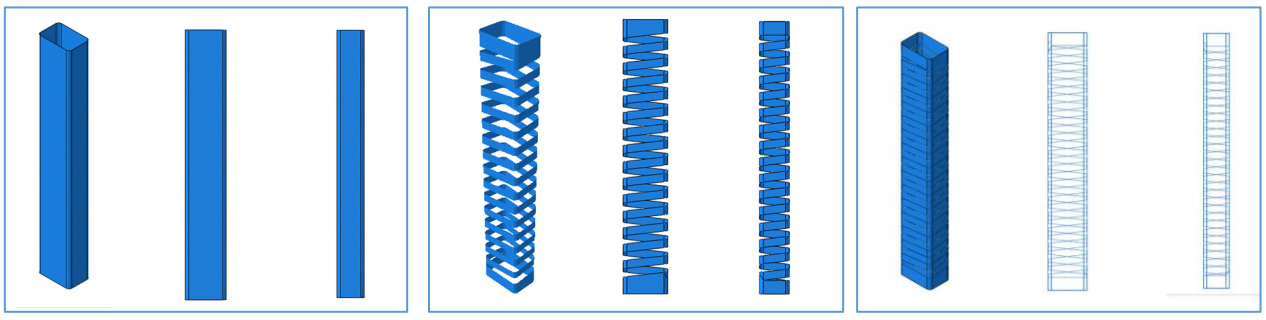

(a) **(b)** **(c)**

Figure 2 – GFRP Installation Details: (a) for the fiberglass cloth, (b) for the fiberglass tape, (c) for the fiberglass tape plus fiberglass cloth

2.2 Specimens modelling

The model was analyzed with finite elements, and the approach adopted in this work is numerical modeling, using the Abaqus/CAE2017 program, where concrete columns are considered as a 3D linear brick by solid elements, rebar as 3D lattice elements, and fiberglass tape and cloth as deformable 3D shell elements. All these parts were created separately and then assembled.

Once the specimen is created and assembled in ABAQUS, boundary conditions are specified to allow interactions between the parts, such as the "Embedded Region Constraint" interaction between the concrete and reinforcing bars, and the "Tie constraint" interaction between the specimen and wrapping elements, whether cloth or tape, because it gives the perfect combination while controlling the surface of the master and slave. Through the displacement control technique, the monotone axial loading applicated to the specimen, where the degree of freedom (DOF) is imposed by moving the top of the shaft by 50 mm as shown in Figure3.

In this work, a concrete damage plasticity model (CDPM) based on plasticity theory and damage mechanics was used to simulate the behavior of concrete, with compression damage values based on the formula of (Kent & Park, 1971) as shown in Figure 5 and with tensile damage values based on the formula of (Massicotte *et al*., 1990) as shown in Figure 6.

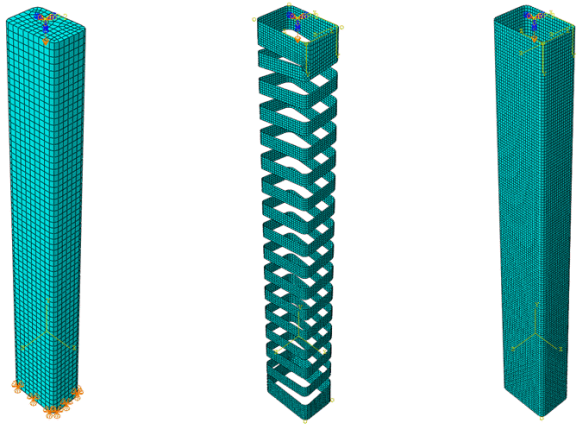

(a) **(b)** **(c)**

Figure 3 – Boundary Condition Model: (a) Column Specimen, (b) fiberglass tape, (c) fiberglass cloth

Figure 4 shows the behavior of the concrete subjected to a uniaxial charge, and the following are the compressive stress-strain model equations which is applied to the Kent and Park model using the modification of (Hafezolghorani *et al*., 2017).

$$\sigma_c = \sigma_{cu}\left[2\left(\frac{\varepsilon_c}{\dot{\varepsilon}_c}\right) - \left(\frac{\varepsilon_c}{\dot{\varepsilon}_c}\right)^2\right] \quad (1)$$

$$250000\,\varepsilon_c^2 - 1000\,\varepsilon_c + \sigma_c/\sigma_{cu} = 0 \quad (2)$$

Where σ_{cu} is the compressive strength of concrete at 28 days, $\dot{\varepsilon}_c$ is the value of the peak strain when the stress reaches σ_{cu}, and ε_c is the strain that occurs.

$$\varepsilon_c{}^{in,h} = \varepsilon_c - \sigma_c/E_0 \quad (3)$$

$$d_c = 1 - \sigma_c/\sigma_{cu} \quad (4)$$

$$E_c = 5000\sqrt{\sigma_{cu}} \quad (5)$$

Where $\varepsilon_c{}^{in,h}$ is the Inelastic strain, d_c is the damage parameter compression, and E_c is the Young's modulus.

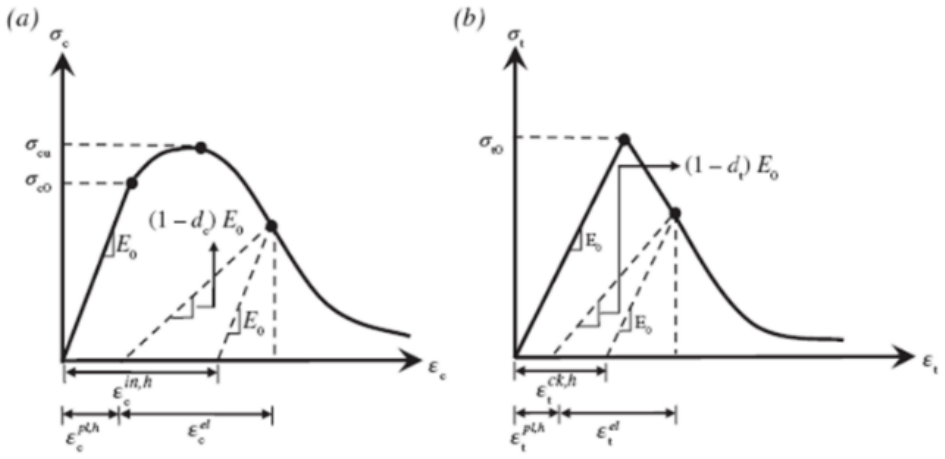

(a) Compression **(b) Tension**

Figure 4 – Concrete's behavior when subjected to uniaxial loading (Hafezolghorani *et al*., 2017)

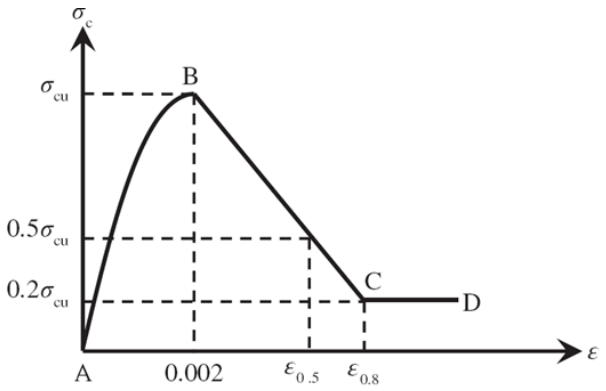

Figure 5 – Model for confined and unconfined concrete (Kent & Park, 1971)

Figure 7 shows the behavior the tension softening curve, and the following are the tensile stress-strain model equations which is applied to the (Massicotte *et al*., 1990) model using the modification of (Allam *et al*., 2013).

$$f_t = 0.7\sqrt{f_{c28}} \tag{6}$$

$$d_t = 1 - \sigma_t/\sigma_{t0} \tag{7}$$

$$\varepsilon_t{}^{ck,h} = \varepsilon_t - \sigma_t/E_0 \tag{8}$$

Where $f_t$the tensile strength of concrete is at 28 days, d_t is the damage parameter, and $\varepsilon_t{}^{ck,h}$ is the cracking strain.

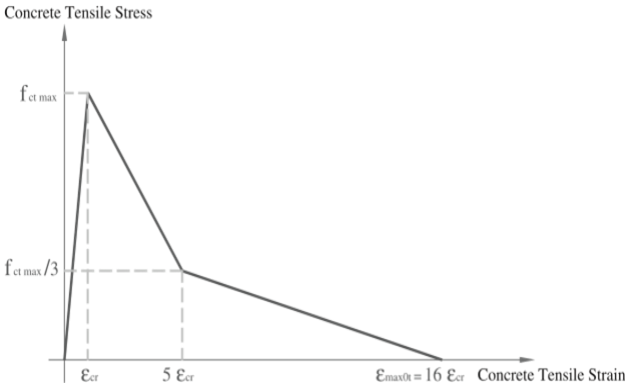

Figure 6 – Tension softening curve suggested by Massicotte *et al*. (1990)

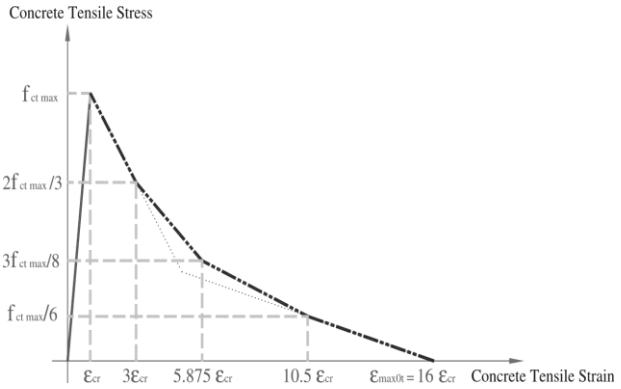

Figure 7 – Tension softening curve modified by Allam *et al*. (2013)

The reinforcing steel properties employed by (Kurniawan *et al*., 2021) were used in this study. And the behavior of fiberglass was modelled using a type elastic linear by a lamina of 0.5 mm according to ABAQUS/CAE User's Manual (ABAQUS, Version 6.7, ABAQUS, Inc. DASSAULT Systems, USA, 2017).

This simulation uses the physical characteristics of the concrete, rebar and fiberglass shown in Tables 2 to 6.

Table 2 – Material properties for concrete.

Concrete elastic			**Plasticity parameters**	
Compressive strength 5 MPa	**Compressive strength 10 MPa**	**Compressive strength 15 MPa**	Dilation angle	30.5
E=11180.339	E=15811.38	E=19364.916	Eccentricity	0.1
			F_{B0}/F_{C0}	1.16
			K	0.67
ν = 0.3	ν = 0.3	ν = 0.3	Viscosity parameter	0.001

Table 3 – Material properties for rebar 12 mm.

Elastic	**Plastic**	
	Yield Stress	**Crushing strain**
E = 184000	400.0	0.000
ν = 0.3	500.0	0.088

Table 4 – Material properties for rebar 6 mm.

Elastic	Plastic	
	Yield Stress	Crushing strain
E = 218000	240.0	0.0000
ν = 0.3	300.0	0.1188

Table 5 – Orthotropic elastic properties of fiber-reinforced epoxy.

E_L /MPa	E_T /MPa	G_{LT} /MPa	G_{TT} /MPa	ν_{TT}	ν_{LT}
55000	9500	5500	3000	0.45	0.33

Table 6 – Orthotropic damage initiation properties of fiber-reinforced epoxy.

$\sigma_L^{f,t}$ /MPa	$\sigma_L^{f,c}$ /MPa	$\sigma_T^{f,t}$ /MPa	$\sigma_T^{f,c}$ /MPa	T_{LT}^{f}
2500	2000	50	150	50

3. Results and discussions

3.1. Load-displacement curves

Table 7 summarizes the simulation findings for the highest axial loads and specimen displacement.

Table 7 – Summary of simulation results.

Specimen	Compressive Strength /MPa	Peak load /KN	Displacement /mm	Strength increases ratio	Percentage increase /%
C1 C	5	374.62	2.97	/	/
	10	697.69	2.97		
	15	1015.80	3.67		
C2 RC	5	531.91	3.67	0.00	00.00
	10	868.73	3.67		
	15	1198.03	3.94		
C3 RC-2T	5	647.10	4.22	1.22	21.66
	10	987.37	3.94	1.14	13.66
	15	1307.07	3.94	1.09	9.10
C4 RC-2 T-2C	5	1179.48	2.97	2.22	121.75
	10	1617.10	2.97	1.86	86.15
	15	1986.55	4.70	1.66	65.82
C5 RC-2T-4C	5	1609.69	2.97	3.03	202.63
	10	2136.62	2.97	2.46	145.95
	15	2600.10	3.67	2.17	117.03

Figure 8 shows the load displacement curves of various types of concrete, including unreinforced concrete specimen, reinforced concrete specimen, glass fiber tape wrapped specimen, and glass fiber tape wrapped specimen with cloth.

The maximum axial load and maximum displacement for the specimen C2/RC reference column are 1198.03 KN and 3.93 mm, respectively. As it is clear from Figure 8 that once the load reaches its maximum, the sample load capacity begins to decrease until the loading is complete.
The column specimen C5/RC-2T-4C has a maximum axial load of 2600.10 KN and a maximum displacement of 3.67 mm. and the curve depicts how the load capacity of the specimen does not diminish when the load reaches its maximum and continues to do so until loading is complete.

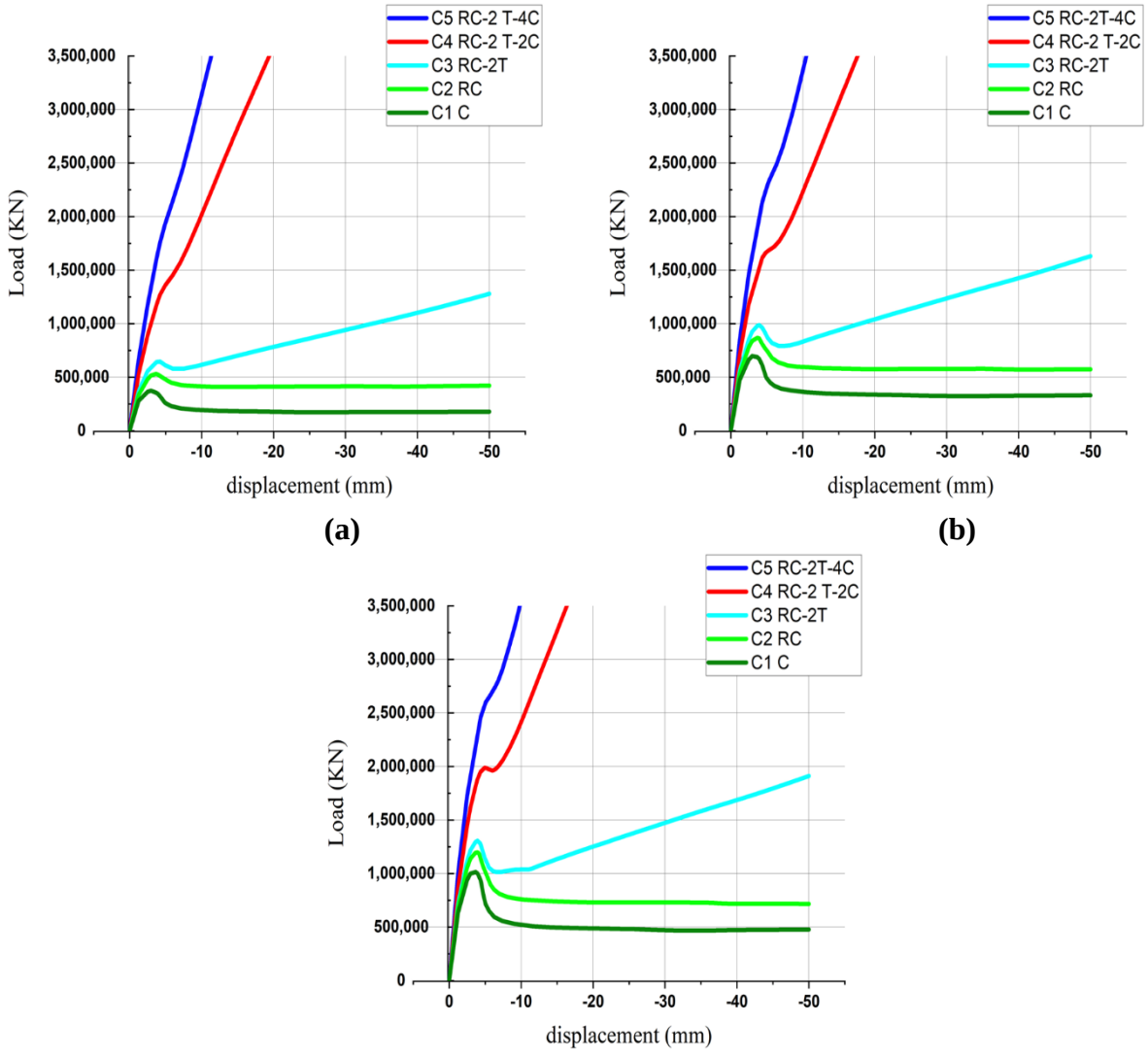

Figure 8 – Load displacement curves of uniaxial load in concrete specimens: (a) with a very low strength 5 MPa, (b) with a low strength 10 MPa, (c) with a low strength 15 MPa

Load displacement curves for three specimens (C3/RC-2T, C4/RC-2 T-2C and C5/RC-2T-4C) represent the most interesting and discussed simulation results. In contrast to other materials, concrete with a very low strength of 5 MPa has the largest percentage increase in load capacity 202.63 %, while concrete with a strength of 15 MPa has the lowest value 117.03 %. The peak load of each concrete type for the simulated specimens is summarized in the graphs in Figures 9, 10 and 11.

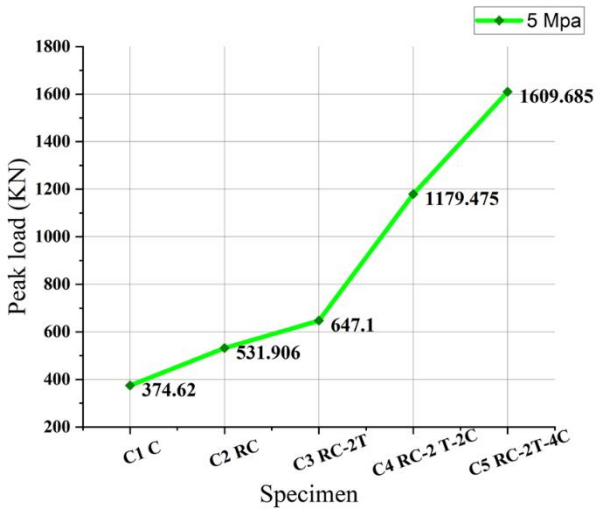

(a) Curve peak load (kN) of concrete with a compressive strength of 5 MPa for different specimens

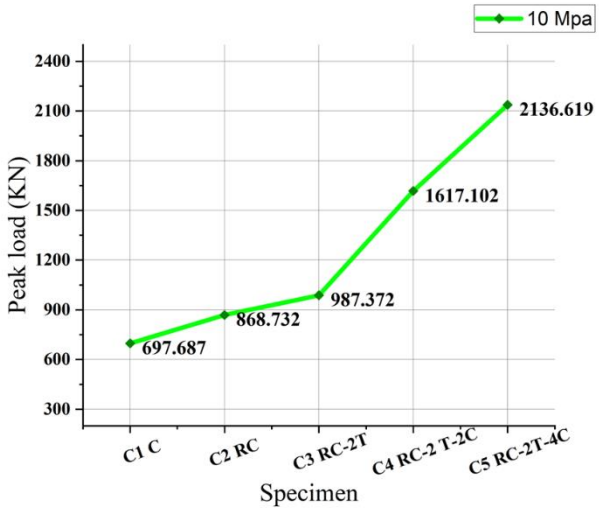

(b) Curve peak load (kN) of concrete with a compressive strength of 10 MPa.

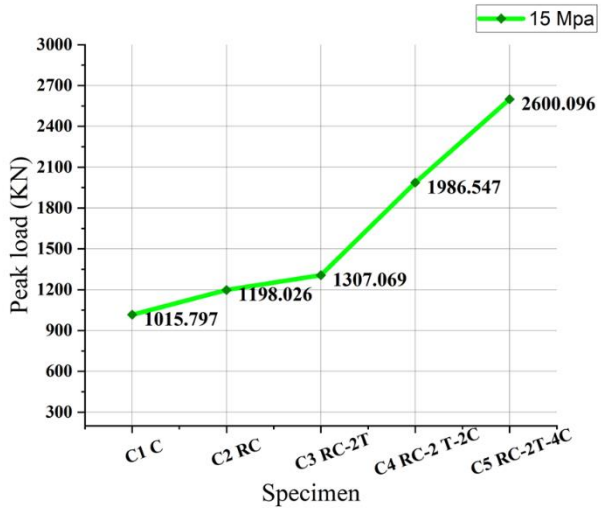

(c) Curve peak load (KN) of concrete with a compressive strength of 15 MPa.

Figure 9 – Curve peak load of uniaxial load

Figure 10 depicts a histogram of the peak load of simulated samples for various types of concrete strength, while Figure 11 depicts a percentage increase curve for various approaches used, including reinforcement by glass fiber tape, fiberglass cloth, and fiberglass tape plus cloth.

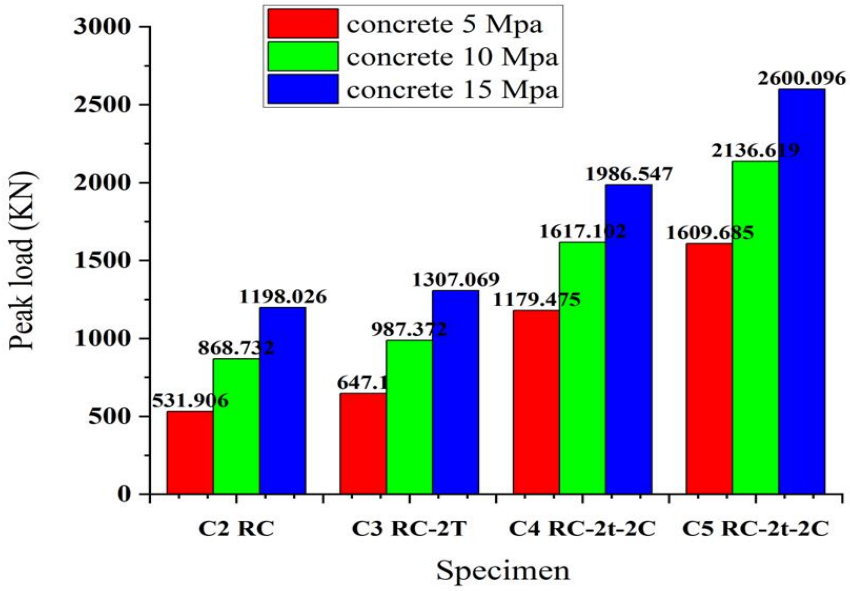

Figure 10 – histogram of the peak load of simulated samples

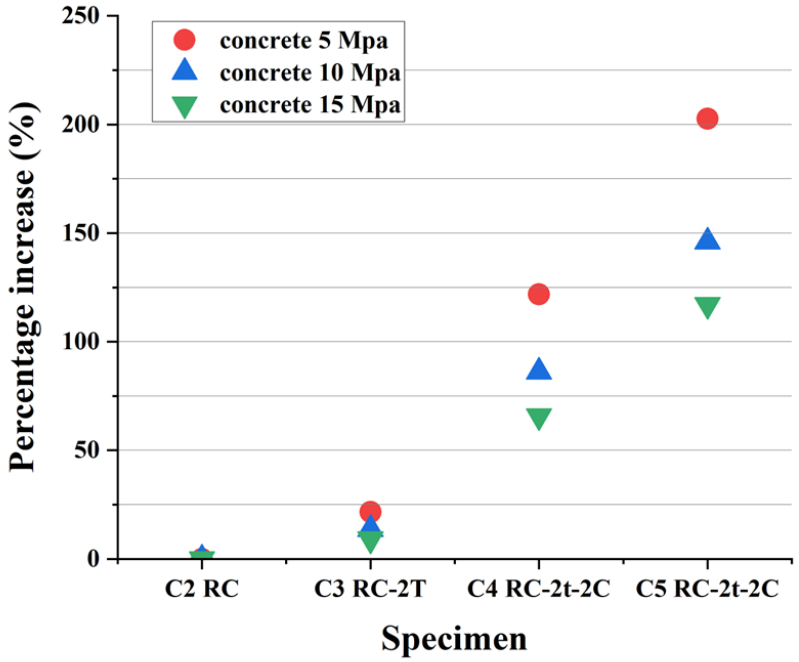

Figure 11 – percentage increase for various approaches used.

3.2. Deformation shapes

The deformed shape of simulated specimens varies depending on the reinforcing technique from one specimen to another, and the strength of the concrete specimen also influences the degree and severity of failure.

The deformed shape of the reinforced concrete specimen used as a reference column, as illustrated in Figure 12 a is dominated by vertical displacement, with the largest stress appearing in the center of the extension to the column base. Because the confinement effect of the shear

reinforcement is plainly visible, the distorted shape of the reinforced specimen is entirely different from that of the reference specimen.

The maximum stress generally occurs at the base of the fully confined column, although the maximum stress for the partially confined column occurred at mid-height as shown in Figure 12 b and Figure 12 c. So, the column fully reinforced with fiberglass shows sufficient behavior compared to the partially reinforced column.

In terms of real stress, the column reinforced with fiberglass cloth outperforms the reinforced concrete column and the column reinforced with fiberglass tape.

It also illustrates that the fiberglass is capable of spreading stresses such that no strain builds in the specific region of the concrete, as evidenced by the color of the outline.

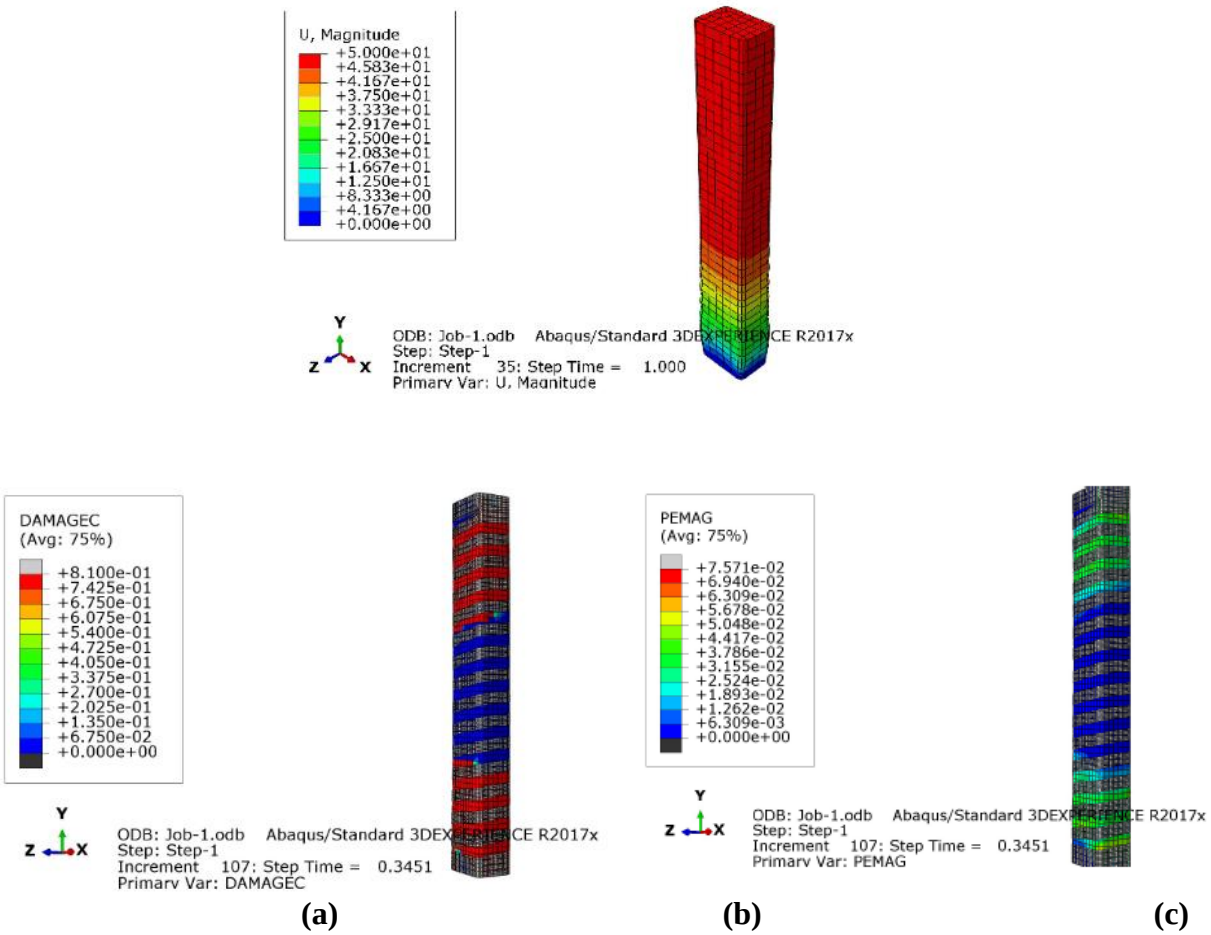

Figure 12 – Uniaxially loaded deformation shapes (DAMAGEC): (a) Reference column, (b) Column reinforced with two layers of fiberglass tape, (c) Column reinforced with two layers of fiberglass tape and four layers of fabric

4. Conclusions

Numerical simulation of reinforced concrete columns reinforced with fiberglass polymer was the focus of this study. Where concrete columns with very low, low, and medium compressive strengths of 5.10 and 15 MPa were used in the models. Two types of confainment are used in this work, the first is a partial confainment made of fiberglass tape and the second is a full confainment made of fiberglass fabric. Based on simulation findings, reinforced concrete completely strengthened with fiberglass tape and cloth has the highest maximum load capacity when compared to reinforced concrete partially strengthened with fiberglass tape. Furthermore, the fiberglass cloth used in the column reinforcement has a considerable influence on enhancing the ductility of the materials. The simulation findings on columns with a 5MPa concrete really offer a pretty accurate

image of the increase in maximum load capacity by more than column specimens with low and medium strength concrete (10 and 15 MPa). The results of this investigation only consider the uniaxial loading of the specimen. In the future, it will be important to investigate how lateral loading affects a material's capacity to support load. The failure behavior of reinforced concrete columns strengthened by fiberglass should also be investigated vis a cyclic loading.

Acknowledgements

This research is supported and funded by Civil Engineering Research Laboratory (LGC-ROI)-Risks and Structures in Interactions, Department of Civil Engineering, Faculty of Technology, University of Batna 2, Algeria as part of the 2022 Research Grants Program.

References

ABAQUS, version 6.7, ABAQUS, Inc. DASSAULT Systems, USA, 2017.

Abdelhamid, F., Yahiaoui, D., Saadi, M., & Lahbari, N. (2022). Lateral Reliability Assessment of Eccentrically Braced Frames Including Horizontal and Vertical Links Under Seismic Loading. *Engineering, Technology and Applied Science Research*, 12(2), 8278–8283. Doi :https://doi.org/10.48084/etasr.4749

Allam, S. M., Shoukry, M. S., Rashad, G. E., & Hassan, A. S. (2013). Evaluation of tension stiffening effect on the crack width calculation of flexural RC members. *Alexandria Engineering Journal*, 52(2), 163–173. https://doi.org/10.1016/j.aej.2012.12.005

Benzaid, R., Chikh, N. E., & Mesbah, H. (2008). Behaviour of square concrete column confined with GFRP composite WARP. *Journal of Civil Engineering and Management*, 14(2), 115–120. https://doi.org/10.3846/1392-3730.2008.14.6

Guettafi, N., Yahiaoui, D., Abbeche, K., & Bouzid, T. (2022). Numerical Evaluation of Soil-Pile-Structure Interaction Effects in Nonlinear Analysis of Seismic Fragility Curves. *Transportation Infrastructure Geotechnology*, 9(2), 155–175. https://doi.org/10.1007/s40515-021-00161-y

Guo, Y. C., Gao, W. Y., Zeng, J. J., Duan, Z. J., Ni, X. Y., & Peng, K. Di. (2019). Compressive behavior of FRP ring-confined concrete in circular columns: Effects of specimen size and a new design-oriented stress-strain model. *Construction and Building Materials*, 201, 350–368. https://doi.org/10.1016/j.conbuildmat.2018.12.183

Hafezolghorani, M., Hejazi, F., Vaghei, R., Jaafar, M. S. Bin, & Karimzade, K. (2017). Simplified damage plasticity model for concrete. *Structural Engineering International*, 27(1), 68–78. https://doi.org/10.2749/101686616X1081

Houda, G., Tayeb, B., & Yahiaoui, D. (2018). Key parameters influencing performance and failure modes for interaction soil–pile–structure system under lateral loading. *Asian Journal of Civil Engineering*, 19(3), 355–373. https://doi.org/10.1007/s42107-018-0033-4

Hussain, Q., Rattanapitikon, W., & Pimanmas, A. (2016). Axial load behavior of circular and square concrete columns confined with sprayed fiber-reinforced polymer composites. *Polymer Composites*, 37(8), 2557–2567. https://doi.org/10.1002/pc.23450

Kent, D. C., & Park, R. (1971). Flexural Members with Confined Concrete. *Journal of the Structural Division*, 97(7), 1969–1990. https://doi.org/10.1061/JSDEAG.0002957

Kurniawan, P., Kasyanto, H., & Mauludin, L. M. (2021). Numerical modeling of low strength reinforced concrete column strengthened with CFRP jacketing. Journal of Physics: Conference Series, 1839 012007. https://doi.org/10.1088/1742-6596/1839/1/012007

Lemsara, F., Bouzid, T., Yahiaoui, D., Mamen, B., & Saadi, M. (2023). Seismic Fragility of a Single Pillar-Column Under Near and Far Fault Soil Motion with Consideration of Soil-Pile Interaction. *Engineering, Technology & Applied Science Research*, 13(1), 9819–9824. https://doi.org/10.48084/etasr.5405

Massicotte, B., Elwi, A. E., & MacGregor, J. G. (1990). Tension-Stiffening Model for Planar Reinforced Concrete Members. *Journal of Structural Engineering*, 116(11), 3039–3058. https://doi.org/10.1061/(asce)0733-9445(1990)116:11(3039)

Nesrine, G., Djarir, Y., Khelifa, A., & Tayeb, B. (2021). Performance assessment of interaction soil pile structure using the fragility methodology. *Civil Engineering Journal (Iran)*, 7(2), 376–398. https://doi.org/10.28991/cej-2021-03091660

Obaidat, Y. T., Ashteyat, A. M., Obaidat, A. T., & Alfaris, S. F. (2020). A new technique for repairing reinforced concrete columns. *Journal of Building Engineering*, 30(1), 1–13. https://doi.org/10.1016/j.jobe.2020.101256

Saadi, M., & Yahiaoui, D. (2022). The Effectiveness of Retrofitting RC Frames with a Combination of Different Techniques. *Engineering, Technology and Applied Science Research*, 12(3), 8723–8727. https://doi.org/10.48084/etasr.4979

Sekhri, K., Yahiaoui, D., & Abbache, K. (2020). Inelastic response of soil-pile-structure interaction system under lateral loading: A parametric study. *Jordan Journal of Civil Engineering*, 14(2), 250–266. https://doi.org/10.1007/978-981-33-6311-3_115

Souheyla, S., & Djarir, Y. (2022). Seismic Vulnerability of Interaction Soil-Pile-pier Bridges Under Mainshock-Aftershock Sequences Using the Fragility Methodology. 5th International Conference of Contemporary Affairs in Architecture and Urbanism journal 904–908. https://doi.org/10.38027/iccaua2022en0084

Tan, K. H., Bhowmik, T., & Balendra, T. (2013). Confinement model for FRP-bonded capsule-shaped concrete columns. *Engineering Structures*, 51, 51–59. https://doi.org/10.1016/j.engstruct.2012.12.039

Yahiaoui, D., Boutrid, A., Saadi, M., Mamen, B., & Bouzid, T. (2023). New Anchorage Technique for GFRP Flexural Strengthening of Concrete Beams Using Bolts-End Anchoring System. *International Journal of Concrete Structures and Materials*, 17(1), 1–15. https://doi.org/10.1186/s40069-023-00578-4

Yahiaoui, D., Mamen, B., Saadi, M., & Bouzid, T. (2022). Experimental Verification Of The New Models Applied To Glass Fibre Reinforced Concrete (Gfrc) Confined With Glass Fibre Reinforced Polymer (Gfrp) Composites. *Ceramics-Silikáty*, 66(3), 384–395. https://doi.org/10.13168/cs.2022.0034

Yahiaoui, D., Saadi, M., & Bouzid, T. (2022). Compressive Behavior of Concrete Containing Glass Fibers and Confined with Glass FRP Composites. *International Journal of Concrete Structures and Materials*, 16(1), 1–19. https://doi.org/10.1186/s40069-022-00525-9

Yang, J., Lu, S., Wang, J., & Wang, Z. (2020). Behavior of CFRP partially wrapped square seawater sea-sand concrete columns under axial compression. *Engineering Structures*, 222, 1–15. https://doi.org/10.1016/j.engstruct.2020.111119

Zeng, J. J., Guo, Y. C., Gao, W. Y., Chen, W. P., & Li, L. J. (2018). Stress-strain behavior of concrete in circular concrete columns partially wrapped with FRP strips. *Composite Structures*, 200, 810–828. https://doi.org/10.1016/j.compstruct.2018.05.001

Zeng, J. J., Guo, Y. C., Gao, W. Y., Li, J. Z., & Xie, J. H. (2017). Behavior of partially and fully FRP-confined circularized square columns under axial compression. *Construction and Building Materials*, 152, 319–332. https://doi.org/10.1016/j.conbuildmat.2017.06.152